



A field test of unconventional camera trap distance sampling to estimate abundance of marmot populations

Authors: Corlatti, Luca, Sivieri, Stefano, Sudolska, Bogna, Giacomelli, Stefano, and Pedrotti, Luca

Source: Wildlife Biology, 2020(4)

Published By: Nordic Board for Wildlife Research

URL: <https://doi.org/10.2981/wlb.00652>

BioOne Complete (complete.BioOne.org) is a full-text database of 200 subscribed and open-access titles in the biological, ecological, and environmental sciences published by nonprofit societies, associations, museums, institutions, and presses.

Your use of this PDF, the BioOne Complete website, and all posted and associated content indicates your acceptance of BioOne's Terms of Use, available at www.bioone.org/terms-of-use.

Usage of BioOne Complete content is strictly limited to personal, educational, and non - commercial use. Commercial inquiries or rights and permissions requests should be directed to the individual publisher as copyright holder.

BioOne sees sustainable scholarly publishing as an inherently collaborative enterprise connecting authors, nonprofit publishers, academic institutions, research libraries, and research funders in the common goal of maximizing access to critical research.



A field test of unconventional camera trap distance sampling to estimate abundance of marmot populations

Luca Corlatti, Stefano Sivieri, Bogna Sudolska, Stefano Giacomelli and Luca Pedrotti

L. Corlatti ✉ (luca.corlatti@wildlife.uni-freiburg.de), Chair of Wildlife Ecology and Management, Univ. of Freiburg, Tennenbacher Str. 4, DE-79106 Freiburg, Germany. – LC, B. Sudolska, S. Giacomelli and L. Pedrotti, Stelvio National Park, Bormio, Italy. – S. Sivieri, Istituto Oikos, Milano, Italy.

The increasing use of remote motion-sensitive photography recently led to an extension of distance sampling (DS) to accommodate camera trap data. Camera trap distance sampling (CTDS) has been proposed as a promising tool to estimate animal abundance, if temporally limited availability for detection is accounted for. However, the performance of CTDS in different field situations, and its reliability when single still images are used instead of videos or bursts of images remain untested. We used Alpine marmots *Marmota marmota* in the Stelvio National Park (Italy) to address three aims: 1) compare estimates of availability bias-corrected CTDS when using single still images with different set-ups to define sampling effort. For the ‘user-manual’ set-up we used values of θ [angle of view] and t^* [recovery time, i.e. the shortest interval at which an animal can be detected] specified by the camera user manual. For the ‘empirical’ set-up we estimated θ and t^* empirically. 2) Compare estimates of CTDS and line DS, both corrected for availability bias based on marmot behavior. 3) Compare estimates of CTDS corrected for availability bias with estimates obtained with capture–mark–recapture (CMR), accounting for the effective trapped area. Our results suggest that: 1) CTDS with ‘user-manual’ set-up underestimated population size compared to the ‘empirical’ set-up; 2) ‘empirical’ CTDS estimates were similar to those of line DS, but CTDS had lower precision; 3) availability bias-corrected CTDS underestimated abundance compared to CMR. Assessing camera settings empirically is crucial to reduce bias in CTDS estimators when single still images are used. Videos should be preferred as they allow choosing predefined snapshot moments and do not rely on settings that cannot be changed. Overall, our results support the use of CTDS as an alternative to DS, although proper availability-bias corrections and many cameras are needed to ensure accuracy and acceptable precision.

Keywords: abundance, availability bias, capture–recapture, *Marmota*, passive monitoring

Estimating spatial and temporal changes in population abundance is a key issue in wildlife research and management (Williams et al. 2002, Fryxell et al. 2014). Investigating the effects of variation in environmental conditions or management strategies, for example, often requires a reliable assessment of associated changes in animal population size in space and/or in time (Yoccoz et al. 2001). Detecting all animals in a given survey, however, is challenging, and not accounting for imperfect detection would return a biased estimator. If the relationship between counted animals and true population size is known, relative abundance indexes may suffice for management or research purposes (Thompson et al. 1998). When the interest is in estimating abso-

lute population size, however, imperfect detection must be explicitly accounted for (Williams et al. 2002).

Several methods have been developed to estimate detection probability in animal populations, either based on marked or unmarked individuals (reviewed by: Seber 1982, Schwarz and Seber 1999, Pollock et al. 2002). Closed capture–mark–recapture (CMR) models are widely used to estimate absolute population size in wildlife studies (Williams et al. 2002), but the costs of marking and resampling animals often make these methods unsuitable for large scale or long-term monitoring. Furthermore, heterogeneity in capture probabilities is a major problem that may bias CMR estimators, if not properly accounted for (Senar et al. 1999, Huggins 2001). Considerable effort has thus been invested in developing methods of abundance estimation that do not require individual identification, including – among the others – multiple observers, N-mixture models and distance sampling (Williams et al. 2002, Greenwood and Robinson 2006). In particular, distance sampling (DS) has found wide application in abundance estimation of several taxa, including birds (Marques et al. 2007),

This work is licensed under the terms of a Creative Commons Attribution 4.0 International License (CC-BY) <<http://creativecommons.org/licenses/by/4.0/>>. The license permits use, distribution and reproduction in any medium, provided the original work is properly cited.

cetaceans (Zerbini et al. 2007), carnivores (Ruelle et al. 2003) and herbivores (Jathanna et al. 2003). Distance sampling inherently accounts for imperfect detection by estimating a detection function $g(x)$ to describe the probability of detecting an animal as a function of its perpendicular distance x from transects or radial distance x from points (Buckland et al. 2001, Thomas et al. 2010). To obtain reliable estimates, various assumptions must be met: all animals on the transect line are detected, animals are randomly and evenly distributed throughout the surveyed area, animals do not move before detection, and measurements (angles and distances) are exact (Buckland et al. 2001, Thomas et al. 2010).

In distance sampling surveys, the probability of detecting animals is often estimated from direct sightings (Buckland et al. 2015), which may be difficult and expensive to perform in remote areas, or when low animal densities reduce sample size for reliable estimation of detection probability (Marques et al. 2013). Over the past years, there has been a growing interest towards the application of passive distance sampling surveys such as sonar, radar and acoustic surveys (Marques et al. 2013, Buckland et al. 2015, Sebastián-González et al. 2018). Compared to human observers, passive monitoring systems allow the automatic collection of a greater amount of data even in remote areas, thus favoring detection of uncommon species. Additionally, they are less sensitive than human observers to factors that affect detection (Marques et al. 2013).

Camera trapping is one of the most widely used passive methods to survey wildlife populations (Rovero and Zimmerman 2016). Several approaches have been proposed to estimate absolute abundance using unmarked individuals trapped by cameras, e.g. N-mixture models (Royle 2004), the random encounter model (Rowcliffe et al. 2008), the spatial count model (Chandler and Royle 2013), and time to event, space to event and instantaneous sampling models (Moeller et al. 2018). Recently, Howe et al. (2017) expanded the use of distance sampling to accommodate camera trap data (camera trap distance sampling: CTDS). The rationale of CTDS is that, when the PIR (passive infrared) sensor of a camera is more likely to detect an animal moving close to the sensor than an animal moving further away from the sensor, a detection function can be fitted to the distribution of distance of animals from the camera. In CTDS, sampling effort can be obtained by discretizing the number of times an animal can be potentially detected over a specified deployment period, using predetermined snapshot moments separated by short time intervals t (e.g. < 3 s). In practice, camera traps should be set in video mode or with long ‘bursts’ of still images, to ensure that animal locations are recorded at times that align with predefined snapshot moments, i.e. every t seconds (Howe et al. 2017).

Capture probability or detection probability (P_{capture} ; $P_{\text{detection}}$) estimated with capture–recapture or distance sampling methods are conditional upon three other probabilities: P_{area} , the probability that the target animals occupy the survey area; P_{presence} , the probability that the target animals occupying the area are present at the time of survey; $P_{\text{availability}}$, the probability that the target animals occupying the area and present at the time of survey are available for detection (Nichols et al. 2009, Schmidt et al. 2017). While P_{area} and P_{presence} can be assumed to be approximately equal to 1 through appropriate sampling design, $P_{\text{availability}}$ and $P_{\text{detection}}$

may be hampered by several factors such as the behavior of the target species, methodological issues, observer experience and habitat complexity (O’Donnell et al. 2015). Under the assumption that individuals are temporarily unavailable at random (i.e. all individuals have an equal probability of being unavailable for capture) during the closed CMR study period, all animals should have a non-negligible chance to be exposed to capture; therefore, probability of availability and detection probability in CMR would be confounded with each other ($P_{\text{availability}} \times P_{\text{capture}}$) (Kendall 1999). CMR models would thus estimate an effective probability of capture for animals in a closed ‘superpopulation’, and the estimated abundance would correspond to the sum of animals that are always available in the survey area, plus those that move in and out of it, or through it (Kendall 1999). Distance sampling methods, on the other hand, are not robust to temporary unavailability, and they return estimates of animals available for detection at any one instant in time (Buckland et al. 2015). If availability is not perfect (i.e. < 1), correction factors should therefore be applied to DS estimates to obtain absolute population size (cf. Buckland et al. 2015). For example, in a recent survey of western chimpanzees *Pan troglodytes verus*, a semiarboreal primate, Cappelle et al. (2019) used the estimates of the proportion of time animals spent active on the ground (or at camera height) to correct the abundance estimates obtained with CTDS. Likewise, Howe et al. (2017) explained that temporally limited availability for detection will always need to be considered and accounted for when using CTDS.

The performance of CTDS, however, remains to be tested in various field situations (Moeller et al. 2018, but see Bessone et al. 2020). Furthermore, although the use of videos or long ‘bursts’ of images is recommended to align observations to predetermined snapshot moments at specific times of day (Howe et al. 2017), researchers and wildlife managers might find this set-up inconvenient and may prefer to use single still images recorded when the camera is triggered (e.g. to maximize battery-life, save space on memory cards or time for data-processing). If single still images are used instead of videos or long ‘bursts’, the chosen interval corresponds to the lowest recovery time t^* between subsequent images. The interval t^* is thus quite different from the definition of t in the CTDS estimator of Howe et al. (2017), and recorded times will hardly align to predetermined snapshot moments at specific times of day, unless recovery time is very short (e.g. < 1 s). The reliability of CTDS when time alignment of observations is violated has never been tested. Furthermore, the use of single images can cause underestimation of the angle of view θ (Rowcliffe et al. 2011) which, in turn, would return a biased estimator. While, with videos, neither t nor θ need to be estimated empirically, CTDS with single still images assumes that proper values of θ and t^* are chosen to define sampling effort. However, the theoretical values of θ and t^* reported in the camera user manual information may not correspond to the realized values of θ and t^* in the field, which can be estimated empirically. Our aim in this paper is thus threefold. 1) After accounting for availability bias using the proportion of time spent being active by animals (cf. Cappelle et al. 2019), we first compare estimates from CTDS using single still images obtained with different set-ups to define sampling effort: ‘user-manual’ versus

‘empirical’, i.e. using theoretical values of θ and t^* specified by the camera user manual information versus values of θ and t^* estimated empirically. 2) We then compare estimates from CTDS corrected for availability bias with estimates from traditional line DS, also corrected for availability bias. 3) Finally, we compare estimates from CTDS corrected for availability bias to estimates obtained with capture–mark–recapture models.

These methods were tested in a population of Alpine marmot *Marmota marmota*, a diurnal, highly social, territorial and semifossorial rodent inhabiting open mountainous areas in central and southern Europe (Armitage 2014). We expect that: 1) ‘user-manual’ and ‘empirical’ availability bias-corrected CTDS estimators should return similar results, under the assumptions that user-manual information is reliable; 2) CTDS and DS estimators corrected for availability bias should return similar results (cf. Howe et al. 2017, Cappelle et al. 2019); 3) after accounting for the effective trapped area, CTDS estimators corrected for availability bias should return similar results to CMR estimators, as both should provide reliable assessment of absolute population size in marmots (cf. Corlatti et al. 2017, Cappelle et al. 2019).

Material and methods

Study area

The study site is located in the Lombardy sector of the Stelvio National Park, Central Italian Alps (46°54'N, 10°41'E)

(Fig. 1) and extends over 37.6 ha on a S–E exposed slope between 2341 and 2671 m a.s.l. Vegetation is mainly represented by alpine and boreal meadows of *Carex curvula* and *Nardus stricta*. The climate is typical of mountainous regions, with harsh winters and mild summers (average temperature ranging from -12°C in January to 23°C in July, own data). To define the boundaries of the study site, we first identified an area with apparently homogeneous marmot distribution, based on preliminary visual observations conducted walking along trails across the area. We then created a minimum convex polygon (MCP) connecting the peripheral main burrows (which corresponded to the locations of the outer traps used for CMR, see description below). Finally, we created a buffer around the MCP, with a span of 83 m, corresponding to the radius of an average home range size for Alpine marmot (~ 2.2 ha: Armitage 2014), to approximate the effective trapped area (see CMR description below). This approach should ensure that P_{area} and P_{presence} are approximately 1 and it should allow a fair comparison between (CT)DS and CMR estimates.

Capture–mark–recapture

Eight occasions of CMR were conducted within one session between 6 and 16 June 2019, soon after the marmots emerged from burrows after hibernation. Two-door Tomahawk's traps ($n=20$) were evenly distributed over the study site (Fig. 1), in close proximity to the main burrows, to maximize the likelihood of capturing individuals. Traps were baited with dandelion flowers *Taraxacum officinalis*, and rebaited after each capture event. Within each occasion, traps

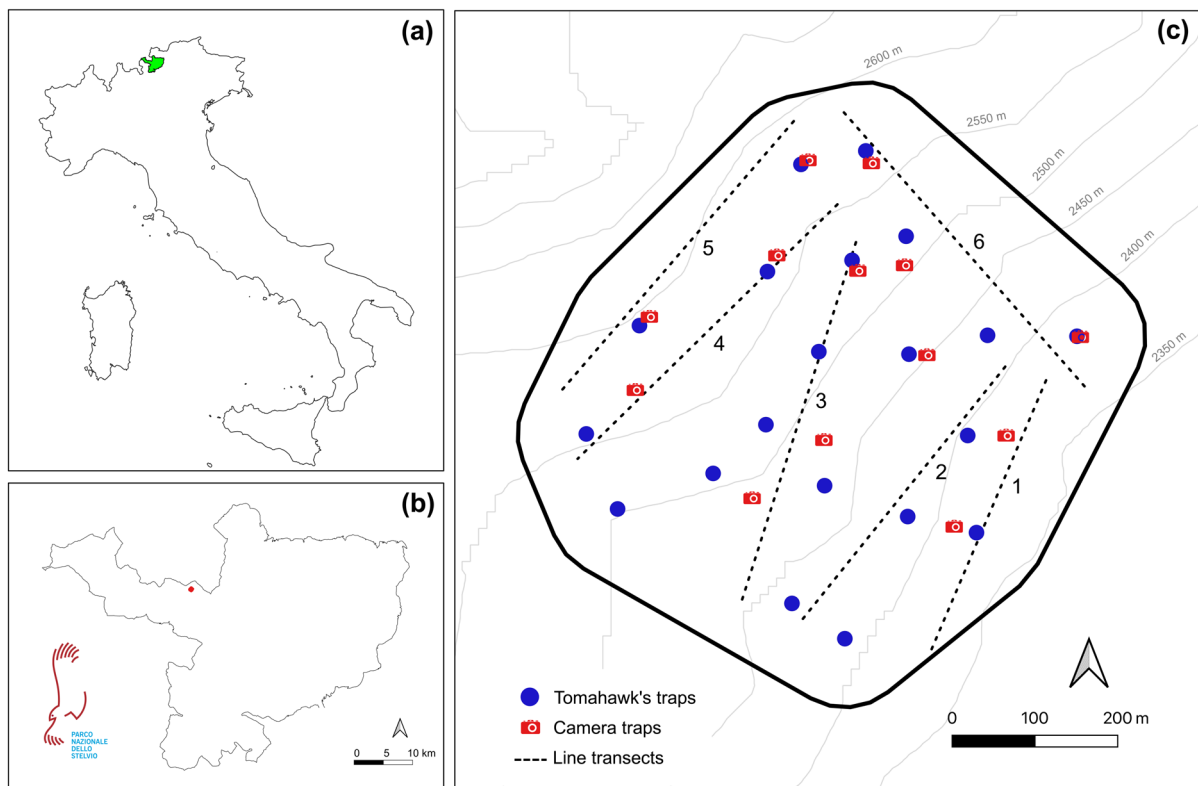


Figure 1. (a) Location of the Stelvio National Park (green area, central Italian Alps); (b) location of the study site (red area) in the north-western part of the Stelvio National Park; (c) distribution of line transects (dashed black lines), camera traps (red cameras) and trapping locations (blue dots) within the boundaries of the study area (continuous black line). In (c), numbers indicate the ID of line DS transects.

were kept open between 08:00 h and 20:00 h, and capturing effort was constant throughout the closed sampling session. Captured individuals were marked permanently by injection of a Tracer Bayer transponder pit and with different combinations of coloured ear-tags. Animals were not sedated and the entire manipulation process always took less than 30 min. Captures were always made with the assistance of a veterinarian, and after receiving authorization from ISPRA (the Italian Institute for Environmental Protection and Research). At the end of the CMR session, an 8-column capture history was built for each individual, based on the occurrence (1/0) of capture–recapture events within each occasion.

Classic CMR modelling suffers an ‘edge effect’, namely the effective area trapped is larger than the trap grid area, and includes the entire home range of animals (White et al. 1982). To reduce the edge effect and approximate the effective trapped area, we created a buffer around the MCP of the trap grid, using the radius of an average home range size for Alpine marmot (Fig. 1c). As in Corlatti et al. (2017), capture data were analysed with the eight closed-population additive models of Otis et al. (1978), which allow for different parametrizations of capture probability: M_0 (uniform), M_t (time-varying); M_b (with behavioural response); M_h (with individual heterogeneity); M_{tb} (time-varying with behavioural response); M_{th} (time-varying with individual heterogeneity); M_{bh} (with behavioural response and individual heterogeneity); M_{tbh} (time-varying with behavioural response and individual heterogeneity). The closure assumption was approximated by the short timeframe used for the primary session of capture (10 days). Data analysis was conducted with a full likelihood approach using the package ‘RMark’ (Laake 2013) with R ver. 3.6.1 (<www.r-project.org>) in R Studio 1.2.5019 (RStudio Team 2019). Individual heterogeneity in capture probability was approximated using 2-mixture modelling (White 2008). The eight models were ranked based on their values of AICc (Akaike’s information criterion corrected for small samples), and averaged to obtain final estimates (Burnham and Anderson 2002).

Availability bias correction

$P_{\text{detection}}$ estimated with distance sampling methods is conditional upon animals being available for detection. $P_{\text{availability}}$ in marmots, is hampered by the semifossorial behavior of the species. Normally, at any one instant in time, only a fraction of the marmots living in the survey area is outside of the burrows, thus only surface-dwelling animals will be available for detection, irrespective of the distance of animals from the transect (i.e. $P_{\text{availability}} < 1$). Correction factors such as the percentage of time spent by animals inside and outside of burrows could be applied to obtain absolute estimates of population size with distance sampling methods. This, however, requires additional field effort or reliable knowledge of the species’ surfacing behavior.

Cappelle et al. (2019) approximated the proportion of animals available for detection using the number of videos obtained per hour, assuming that at the peak of their activity all animals were available for detection. More generally, under the assumption that at the peak of the daily activity cycle all animals are active, the proportion of active time corresponds to the ratio between the area under the activity curve (AUC)

and the area within the rectangle defined by the maximum of the curve (AUR) (Rowcliffe et al. 2014). This approach was adopted to estimate $P_{\text{availability}}$ in our study, assuming that the proportion of time spent being active approximates the proportion of time spent by marmots being outside of burrows (i.e. being available for detection).

Marmot activity cycle was assessed using time data converted to radians, extracted from still images collected between 23 and 30 June 23 during CTDS (see the description of CTDS data collection). We used a 30-min interval between pictures to consider events as independent (cf. Rovero and Zimmermann 2016). Activity density was estimated by fitting a circular normal distribution to the data with von Mises kernel using the R package ‘overlap’ (Ridout and Linkie 2009). In its basic form, this function returns a mean value for activity density. To estimate uncertainty, 1000 non-parametric bootstrap samples were generated with replacement from the original dataset, and the same kernel function was applied iteratively (cf. Fig. 2). For each bootstrap sample i ($1 < i < 1000$), the proportion of time spent being active by animals within the timeframe of distance sampling data collection was calculated as AUC_i/AUR_i in the time interval 08:00–20:00 h (cf. Fig. 2), using the R package ‘pracma’ (Borchers 2019). Mean and SE for the proportion of active time were extracted from these 1000 values (Rowcliffe et al. 2014), and used to correct the estimates obtained with CTDS and line DS. Specifically, the mean abundance and SE estimated with CTDS and line DS were divided by the estimated mean and SE of the proportion of time spent being active in the interval 08:00–20:00 h, using the R package ‘propagate’ (Spiess 2018), which allows for uncertainty propagation using higher-order Taylor expansions and Monte Carlo simulations.

Camera trap distance sampling

Point transect distance sampling with camera traps was conducted between 23 and 30 June. A total of 13 cameras (ScoutGuard SG-560C) were randomly deployed over the study area (Fig. 1c). Random points were generated within the boundary of the study site with a Geographic Information System software (QGIS ver. 3.8, <<http://qgis.osgeo.org>>), setting the minimum distance between points at 50 m. Each camera was mounted at a height of ca 0.4 m, a value that should represent a good compromise between reducing the possibility that marmots pass beneath the camera at short distances, and the possibility to detect distances over which animals could be detected. Cameras were mounted with the same orientation N–W (cf. Howe et al. 2017), and set at medium sensitivity. Radial distances of photographed marmots from the camera were initially estimated by comparing their locations to those of markers placed at fixed distances (1, 3, 5, 7 and 9 m) along the midline of the camera field of view (Fig. 3) (cf. Hofmeester et al. 2017). Then, observations between 0–1, 1–3, 3–5, 5–7, 7–9 m and beyond were binned, as measurements became imprecise at larger distances. CTDS requires the calculation of sampling effort at each camera point k , i.e. the number of snapshot moments weighted by the fraction of a circle covered by the camera. Sampling effort was defined as $e_k = \frac{\theta T_k}{2\pi t}$ where θ was the angle covered by the camera (in radians), T_k the period of

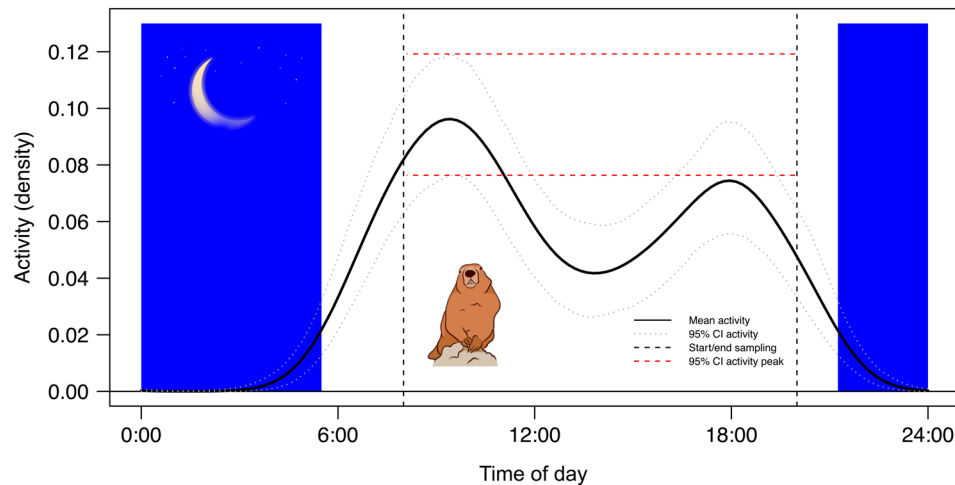


Figure 2. Kernel density estimate (with bootstrap 95% CI for the 95th percentile) of daily activity cycle of marmots in the study area in June 2019. Vertical dashed black lines indicate the timeframe (08:00–20:00 h) used for estimating availability and collecting data with distance sampling and CMR methods; horizontal dashed red lines indicate the estimated uncertainty of activity peak. Blue bars represent night hours.

camera deployment, t the unit of time used to determine a finite set of snapshot moments within T_k (Howe et al. 2017). In this study, the value of t was approximated by t^* , i.e. the lowest non-zero interval between single still images allowed by the camera. It is worth recalling that recovery time t^* is conceptually quite different from t defined in Howe et al. (2017), as the recorded times using t^* will hardly align to predetermined snapshot moments at specific times of day.

First, the period of deployment T_k was defined as the total sampling time (in seconds) at camera k between 23 and 30 June, assuming that daily sampling time was restricted between 08:00 h and 20:00 h. The sampling time between 20:01 h and 07:59 h was excluded a priori from analysis for two reasons: first, marmots are diurnal animals, and they spend their nights in burrows, thus they are unavailable for detection during nighttime (cf. Fig. 2); second, the timeframe 08:00–20:00 h corresponds to the time of data collection with line DS, thus ensuring full comparability between distance sampling methods. For each camera, T_k was calculated from one hour after deployment, to allow for marmots' habituation to the presence of the device, until one hour before displacement, to avoid potential bias caused by the presence of the operator (Howe et al. 2017). Distance data were censored accordingly, and modelled with two different set-ups, 'user-manual' and 'empirical'. For the 'user-manual' set-up, θ was assumed to be 52° (0.908 radians) and t^* was assumed to be 5 s, i.e. the theoretical values specified by the user manual information. For the 'empirical' set-up, θ and t^* were estimated empirically: θ was assessed by walking in front of the camera, perpendicularly to the midline of the field of view, and measuring the distance from the operator to the midline that triggered the PIR sensor, using the camera in setup mode. This procedure was repeated 10 times (walking five times from the left and five times from the right) at different perpendicular distances (5 and 10 m); the angle of view was calculated for each of the 20 trials using basic trigonometric formulas, and its mean value used as an estimate for realized θ . As the interval between images triggered by motion should be affected by distance (owing to missed detections with increasing distance from the camera), the 'empirical' value of t^* was defined as the

shortest interval between images taken by walking randomly in front of the camera at different distances between ca 0.5 and 10 m, for 5 min, keeping the camera recovery time set at 5 s (as in the 'user-manual' set-up). Finally, for both set-ups, detection was modelled with conventional distance sampling using the same functions of Howe et al. (2017): half-normal with 0, 1 or 2 Hermite polynomial adjustment terms; hazard rate with 0, 1 or 2 cosine adjustments; uniform with 1 or 2 cosine adjustments.

To obtain final estimates, models were first ranked according to their information criterion values. Violations of the independence assumption of CTDS data would introduce overdispersion (Howe et al. 2019) and, under these circumstances, AIC (Akaike's information criterion) is likely to select overly complex models (Buckland et al. 2001). Howe et al. (2019) recently proposed a more robust two-step model selection procedure based on: 1) the selection of the models with the lowest value of QAIC (quasi-AIC) within each key function, where the overdispersion parameter (\hat{c}) is calculated from χ^2/df , i.e. the ratio between the χ^2 statistics of the most parametrized model for each key function and its degrees of freedom; 2) the choice of the lowest χ^2/df value across QAIC-selected models. When the estimate of \hat{c} is \leq or equal to 1, the traditional AIC model selection approach should be justified. Models were considered competitive if they had $\Delta(\text{QAIC}) \leq 2$ and non-significant p-values for the χ^2 goodness-of-fit test, and they were averaged to obtain final estimates (Burnham and Anderson 2002). Final estimates of population size within the assumed effective trapped area were obtained correcting averaged mean and SE by the availability bias estimates, accounting for uncertainty propagation.

Line distance sampling

Line transect sampling was conducted between 2 and 7 July 2019. A total of six linear transects, with an average length of 430 m (± 43 SD), were placed according to an opportunistic design that allowed to safely walk the study site, while ensuring homogeneous coverage of the area (Fig. 1c). Transects



Figure 3. Distance of marmots from the camera trap was estimated by comparing animal locations to those of markers placed at fixed distances (1, 3, 5, 7 and 9 m) along the midline of the camera field of view. Data were binned over the same distance intervals. In (a) the animal does not appear to be affected by markers; in (b) the animal seems to show positive behavioral response.

could not be distributed randomly due to the ruggedness of the terrain. This form of opportunistic design, however, is unlikely to bias the estimator, as the visibility from the transects ensured full coverage of the study site. Over the survey period, transects were walked sequentially from 1 to 6 (Fig. 1c). Each transect was walked once per day over five consecutive days (except for one transect, which was walked only on four days) to increase encounter rate, by the same operator (SV), for an overall effort of 12.5 km. Each survey took about 3 h to complete data collection, and surveys were conducted between 08:00 h and 20:00 h. Perpendicular distances to each individual (or groups of individuals) from the transects were collected with a laser rangefinder. Although transects were fairly close to each other, possibly increasing the chance of observing the same animals, double counts, per se, are not a cause of bias if such counts correspond to different transects (Buckland et al. 2001). To analyze the data, estimation was performed using conventional distance sampling without covariates (cf. Corlatti et al. 2017) weighing by stratum effort, since one transect was replicated 4 times instead of 5. We started from uniform, half-normal and hazard-rate key functions, adding cosine adjustment terms to the models until there was no improvement in AIC (Buckland et al. 2001).

Fitted models were ranked based on their AIC values and validated using the χ^2 goodness-of-fit test. As in CTDS, models were considered competitive if they had $\Delta AIC \leq 2$ and non-significant p-values for the χ^2 goodness-of-fit test, and they were averaged to obtain final estimates (Burnham and Anderson 2002). Final estimates of population size within the assumed effective trapped area were obtained correcting averaged mean and SE by the availability bias estimates, accounting for uncertainty propagation.

For both CTDS and line DS, detection functions and abundance were estimated with the R package 'Distance' (Miller et al. 2019).

Results

Capture-mark-recapture

During capture-mark-recapture, we had a total of 70 capture events with 48 individually marked animals. The 'best' model was M_0 (Table 1), but inference was made on the full list of eight models. Model averaging returned an estimate of $n=76$ individuals within the assumed effective trapped area, with 95% CI between 60 and 120, and a CV of 18% (Fig. 5).

Availability bias correction

Marmots were particularly active in the morning, between 08:00 h and 11:00 h, with a second lower peak of activity in the afternoon, between 17:00 h and 19:00 h. No marmots were photographed during night hours (Fig. 2). Availability bias correction assumes that the proportion of time active equals the probability of availability. The estimated mean proportion of time spent being active by marmots between 08:00 h and 20:00 h was 0.67. The estimated SE for active time, obtained with bootstrap resampling, was 0.074. These values were used to correct distance sampling estimators for availability bias.

Camera trap distance sampling

In the time interval 08:00–20:00 h we collected a total of 417 photos with marmots in them, and for each photo we

Table 1. Model selection estimates for the eight capture-mark-recapture models of Otis et al. (1978) fitted to investigate absolute abundance of Alpine marmot in the study site within the Stelvio National Park in June of 2019. The table reports values of Akaike's information criterion corrected for small sample size (AICc), delta AICc values from the best model ($\Delta AICc$), Akaike's weights (Weight), number of parameters (Num. par.) and deviance. All models were selected for averaging.

Model	AICc	$\Delta AICc$	Weight	Num. par.	Deviance
M_0	61.61	0.000	0.643	2	50.971
M_b	63.59	1.984	0.231	3	50.923
M_h	65.68	4.074	0.084	4	50.971
M_{bh}	67.69	6.080	0.031	5	50.923
M_t	73.28	11.670	0.002	9	48.190
M_{tb}	74.46	12.851	0.001	10	47.263
M_{th}	77.50	15.898	0.000	11	48.190
M_{tbh}	77.69	16.085	0.000	12	46.246

Table 2. Camera (point transect) models fitted to estimate available marmot abundance in the study area within the Stelvio National Park in June 2019. The table reports angles of view assumed for the cameras (θ , in degrees), unit of time used to determine the shortest distance between single still images (t^* , in s), key functions (Key), adjustment types (Adj.: –=no adjustment; Cos=cosine), orders of adjustment (Order), Akaike information criterion values (AIC), delta-AIC values from the best model (Δ AIC), significances of χ^2 goodness of fit test (χ^2 -p), abundance estimates (N) with standard error (SE), coefficients of variation (CV). In bold, models selected for averaging.

θ	t^*	Key	Adj.	Order	AIC	Δ AIC	χ^2 -p	N	SE	CV
52°	5	Half-normal	–	–	555.49	0.00	0.464	6	2.01	0.32
		Uniform	Cos	2	555.61	0.12	0.727	7	2.57	0.34
		Half-normal	Herm	3	557.03	1.54	0.799	9	3.35	0.39
		Hazard-rate	Cos	2	557.04	1.55	0.781	9	3.22	0.37
		Uniform	Cos	3	557.04	1.55	0.781	9	3.33	0.39
		Half-normal	Herm	2	557.27	1.78	0.311	6	2.12	0.34
		Hazard-rate	Cos	3	558.96	3.47	NA	8	4.38	0.57
		Hazard-rate	–	–	575.42	19.93	<0.001	4	1.24	0.33
		Half-normal	–	–	555.49	0.00	0.464	20	6.47	0.32
		Uniform	Cos	2	555.61	0.12	0.727	24	8.29	0.34
42°	13	Half-normal	Herm	3	557.03	1.54	0.799	28	10.79	0.39
		Hazard-rate	Cos	2	557.04	1.55	0.781	28	10.36	0.37
		Uniform	Cos	3	557.04	1.55	0.781	28	10.74	0.39
		Half-normal	Herm	2	557.27	1.78	0.311	20	6.82	0.34
		Hazard-rate	Cos	3	558.96	3.47	NA	25	14.10	0.57
		Hazard-rate	–	–	575.42	19.93	<0.001	12	4.00	0.33

recorded the distance between animals and cameras. The theoretical values of θ (52°, 0.908 radians) and t^* (5 s) reported in the user manual were not reliable, since field tests suggested a realized θ of 42° (0.733 radians) and a realized t^* of 13 s. Consequently, the realized mean encounter rate (mean number of marmots photographed per 13-s time interval) across all cameras was 0.002 ± 0.002 SD. We had difficulties in data collection because of the malfunctioning of some cameras: one camera failed after one day of data collection and was not considered for analysis. One camera failed after two days and the pole of another camera was bent by cows after five days. For the two latter cameras, we included in the analysis only the data collected before the last picture was taken or the pole was bent, censoring the sampling effort accordingly. Exploratory analysis revealed other data collection issues. A large portion (about 55%) of the dataset consisted in observations above 9 m and up to 50 m, well outside the range of the camera sensors (< 20 m). The fact that detections increased in the last bin resulted in poor model fit, and we right-truncated data at 9 m (cf. Buckland et al. 2015). As the \hat{c} calculated from χ^2/df returned values < 1 for all the most parametrized models within each key function, the use of AIC for model selection should be justified. The lowest AIC value was returned by a model assuming a half-normal detection function with no adjustments (Table 2, Fig. 4a), but several models had delta AIC within 2 (Table 2). For $\theta=52^\circ$ and $t^*=5$ s, the averaged model returned an abundance of seven marmots within the assumed effective trapped area, with SE of 2.64 and a CV of 36%, while for $\theta=42^\circ$ and $t^*=13$ s, the averaged model returned an abundance of 24 marmots, with SE of 8.51 and a CV of 36%. After correcting for availability and uncertainty propagation in the estimate, for $\theta=52^\circ$ and $t^*=5$ s we obtained an abundance of 11 individuals within the assumed effective trapped area, with 95% CI between 3 and 19 and a CV of 39% (Fig. 5); for $\theta=42^\circ$ and $t^*=13$ s we obtained an abundance of 36 individuals with 95% CI between 11 and 64 and a CV of 37% (Fig. 5).

Line distance sampling

Over all replicates of line transect DS we collected a total of 108 observations ($n=122$ marmots), with an expected group size of $1.12 (\pm 0.05 \text{ SE})$. The average number of

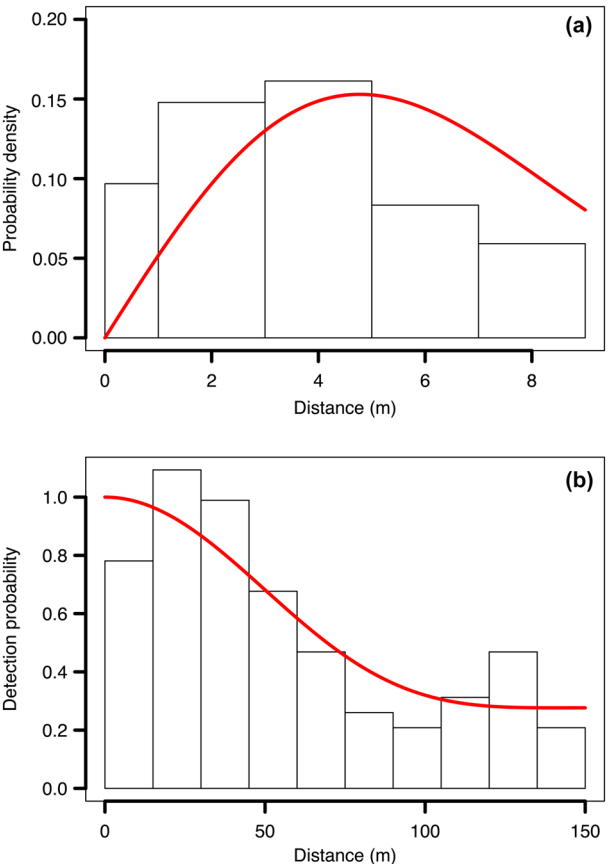


Figure 4. (a) Probability density from half-normal detection function without adjustments, returned by the best fitting model for the distances collected with CTDS in June 2019; (b) uniform detection function with 2 cosine adjustments, returned by the best fitting model for the distances collected with line DS in June–July 2019.

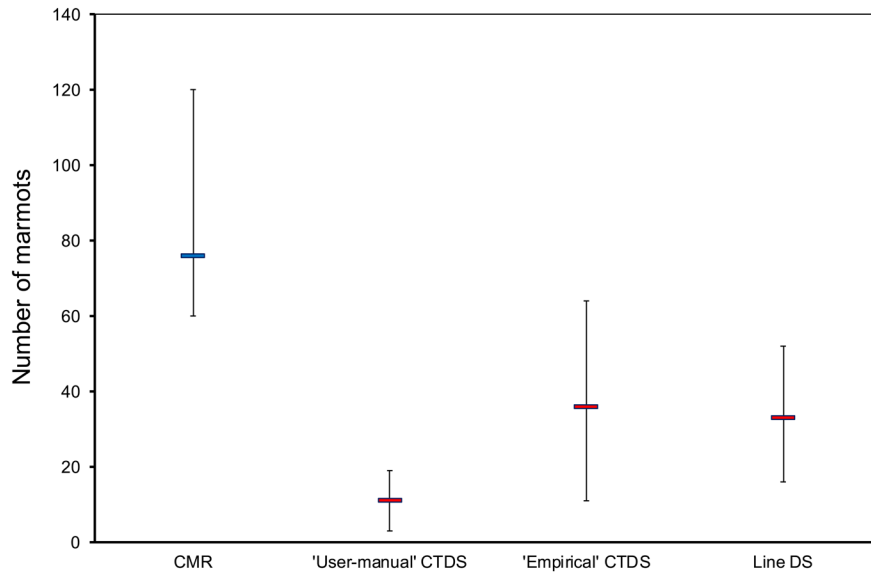


Figure 5. Abundance estimates of the marmot population in the study site within the Stelvio National Park, obtained using different methods (CMR, availability bias-corrected 'user-manual' CTDS, availability bias-corrected 'empirical' CTDS, availability bias-corrected line DS) in June–July 2019. Blue marker indicates the CMR point estimate, red markers point estimates obtained with distance sampling methods. Vertical lines represent 95% confidence intervals.

observations per replicate was $21.6 (\pm 4.39 \text{ SD})$. Distance data were right-truncated at the 5% of the largest observations (Buckland et al. 2001). The model assuming a uniform detection function with 2 cosine adjustments (Fig. 4b) had the lowest value of AIC, but nearly all other models had delta AIC within 2 (Table 3). Model averaging yielded an abundance of 22 marmots within the assumed effective trapped area, with SE of 5.59 and CV of 25%. After correcting for availability and uncertainty propagation in the estimate, we obtained an abundance of 33 individuals with 95% CI between 16 and 52 and a CV of 28% (Fig. 5).

Discussion

Camera traps are increasingly used in wildlife monitoring for different purposes. When the interest is in assessing population size, testing the reliability of statistical methods under different field conditions is necessary to avoid biased estimators (Moeller et al. 2018). In this study we aimed to explore the reliability of an unconventional application of camera trap distance sampling, where single still images instead of videos or long 'bursts' of images were used (cf. Howe et al.

2017). Our results showed that, 1) when the theoretical values provided by the user manual information were used to set θ and t^* , CTDS severely underestimated abundance compared to CTDS with values of θ and t^* estimated empirically. 2) 'Empirical' CTDS yielded estimates of abundance similar to those obtained with traditional line distance sampling, albeit the precision of CTDS estimator was poor. 3) Despite correcting for availability bias, CTDS and line DS severely underestimated population size compared to capture–mark–recapture, within the assumed effective trapped area.

Properly assessing sampling effort is crucial when CTDS is used. An appropriate value for t (interval between snapshot moments), for example, is necessary to define the number of times an animal can be potentially detected. Howe et al. (2017) recommended to choose values of $t < 3$ s and to set cameras in video-mode, as this would allow to align recorded images with pre-specified snapshot moments. When using single still images instead of videos, however, it is not possible to define intervals of time t that allow to align recorded images with specific snapshot moments. The reliability of CTDS when using the recovery time t^* (the shortest interval at which an animal can be detected) instead of t (sensu Howe et al. 2017) to assess sampling effort has never been

Table 3. Line transect models fitted to estimate available marmot abundance in the study area within the Stelvio National Park in July 2019. The table reports used key functions (Key), adjustment types (Adj.: –=no adjustment; Cos=cosine), orders of adjustment (Order), Akaike information criterion values (AIC), delta AIC values from the best model (ΔAIC), significances of χ^2 goodness of fit test ($\chi^2\text{-p}$), abundance estimates (N) with standard error (SE), coefficients of variation (CV). In bold, models selected for averaging.

Key	Adj.	Order	AIC	ΔAIC	$\chi^2\text{-p}$	N	SE	CV
Uniform	Cos	2	1031.43	0.00	0.420	21.7	5.06	0.23
Half-normal	Cos	2	1031.98	0.55	0.417	24.0	5.80	0.24
Half-normal	Cos	3	1032.37	0.94	0.516	21.5	5.69	0.26
Hazard-rate	–	–	1032.44	1.01	0.353	21.0	5.48	0.26
Hazard-rate	Cos	2	1032.46	1.03	0.437	23.4	6.03	0.26
Uniform	Cos	3	1032.96	1.53	0.361	23.5	5.87	0.25
Half-normal	–	–	1035.07	3.64	0.170	18.4	3.96	0.22

tested. In our study, the lowest non-zero value of t^* provided by the camera user manual information (5 s) turned out unrealistic, as the value of t^* estimated empirically was much larger (13 s). This inconsistency had major consequences on the final CTDS estimates, as shorter time intervals increased sampling effort, thereby lowering abundance estimates. Our results highlight the importance of testing for the realized value of t^* in the field, when using single still images.

Despite the outlined shortcomings of using the values provided in the camera user manual and the strength of our estimation approach, also some bias could derive from our estimation of t^* , which could be better defined as the shortest interval between images taken by walking in front of the camera at consistently short distances (i.e. 0.5 m). Furthermore, the empirical value of t^* estimated in this study was likely too long for use in CTDS: conceptually, in point transect snapshot moments should be independent of when an animal enters the detection sector. In CTDS, when the snapshot moments are triggered by a camera detection, to avoid bias, the time between snapshots should be shorter than the shortest time for an animal to pass through the sector (Howe et al. 2017). Also, predetermining moments at specific times of day makes the moments independent of the exact time when animals trigger the sensor. A time of 13 s may have resulted in two types of bias. One is bias towards having a snapshot moment when an animal was present (because it triggered the moment): according to Howe et al. (2017), ‘observed distances upon first detection are expected to be positively biased because animals entering the detection zone through the arc of the sector would contribute a disproportionate number of observations at far distances. Bias would be slight if the time between snapshot moments (t) was small enough to ensure that the animals did not move far relative to the range of the sensor between snapshots’. The second potential bias is that animals may have passed through the sector without detection between snapshot moments. While the first bias will lead to overestimation, the second will lead to underestimation, but there is no guarantee that, in our study, they were of similar magnitude and canceled each other out.

Next, inconsistencies between the ‘user-manual’ and ‘empirical’ values for the angle of view θ (i.e. theoretical versus realized θ in the field) can also bias the estimator, as density decreases with increasing θ (Rowcliffe et al. 2011). This, in turn suggests that the use of a single pre-defined θ value for all cameras might be a source of bias if camera sites have highly heterogeneous environmental conditions, as it is often the case in many field surveys. Furthermore, the ability of camera sensors to detect moving animals may vary depending on camera type and placement, animal size, air temperature and humidity (Hofmeester et al. 2017). While these parameters were likely to be fairly homogeneous in this study, more generally the consequences of their temporal and spatial variations on abundance estimation when CTDS with single still images is used deserve future investigation.

The reliability of estimates crucially relies on the possibility to meet all the assumptions underlying each estimator. In our study, ‘empirical’ CTDS and line DS yielded very similar point estimates, but the precision of CTDS estimator was poor. Interestingly, despite long intervals of time t^* do not allow recorded images to align with specific snapshot moments, our findings are in line with the results obtained

by Capelle et al. (2019). We argue that CTDS is unlikely to have violated the assumption of random distribution of transects with respect to marmot density, as cameras were placed randomly across the study area (Thomas et al. 2010). The key assumption of perfect detection at distance zero ($g(0) = 1$) is difficult to fulfill when surveying small mammals: the need to mount the device at a given height above the ground to allow for the measurement of distances, likely hampers the probability of detecting animals beneath the camera. On the other hand, the use of passive monitoring systems such as camera traps should reduce the negative response of animals to the presence of observers (cf. Marques et al. 2013). However, animals may exhibit complex responses to camera traps, including avoidance or attraction (Séquin et al. 2003), possibly leading to biased encounter rates. Similarly, the use of markers to estimate distance of individuals from the transect might trigger some form of behavioral response in animals (Hofmeester et al. 2017). If this were the case, the availability of marmots for detection, as well as the distribution of distances might be altered, and may possibly bias the estimators. Preliminary work conducted in 2018 in the same study area using camera traps without the presence of markers suggests very similar trapping rates (3.5 marmots day⁻¹ in 2018 versus 3.6 marmots day⁻¹ in this study). Furthermore, marmots did not generally show behavioral response to markers (Fig. 3a), with a few exceptions (Fig. 3b). Therefore, we deem unlikely that, in this study, CTDS estimators were severely biased by the behavioral response of animals. Next, regarding the assumption that distance measurements are exact, we admit that our estimation of distance of detected marmots from the camera was imprecise, but grouping distances within a given interval (binning) should not cause major loss of precision in the estimator of the detection function (Buckland et al. 2015). To obtain sensible detection functions we truncated a large fraction of camera trap data, which showed an increase in frequency in the last bin, likely due to the triggering effect of thermal currents, common in alpine environments. It is unclear to which extent this caused bias in the estimator; however, most of these detections were beyond the range of camera sensors, thus it seems unlikely that truncation caused major violation of model assumptions. Line DS violated the assumption of perfect detection on the transect line (detection probability was about 0.8, Fig. 4b). Most important, while the good visibility in our study area should allow to detect animals from far distances before any movement occurs, the marmot’s antipredatory behavior (alarm calls: Armitage 2014) may have caused movements of available animals away from the observer or triggered burrowing behavior of animals closer to the observer. If so, $P_{\text{detection}}$ and $P_{\text{availability}}$ should decrease at distance zero or close to zero, thereby leading to low estimates (Buckland et al. 2015, Schmidt et al. 2017). Disturbance to marmots might have been exacerbated by walking the transect sequentially on such a small area. Furthermore, conventional line transect sampling may not be the most suitable technique for sampling small areas, as the low number of transects may lead to poor estimates of variance and the maximum detection range (w) may potentially overlap between transects (Buckland et al. 2007).

Capture–recapture methods may be used to estimate population size in marmots with no need for correction

factors (cf. Corlatti et al. 2017). The semifossorial behavior generates a form of temporary emigration sensu Kendall (1999) which would bias estimators if the CMR study period was shorter than the time marmots spend in burrows, because animals in dens would not be available for capture. Capture occasions, however, were conducted over several days, and during daytime hours animals often move in and out of dens. We thus believe that such movements could be considered approximately random and that all individuals had a non-negligible chance to be available for capture during the closed CMR period. Under these assumptions, closed CMR models should be robust to this form of temporary unavailability (Kendall 1999), and the estimated closed ‘superpopulation’ should approximate the number of marmots present in the study area, i.e. the number of marmots present in and out of dens at any given point in time (cf. Corlatti et al. 2017). Admittedly, the number of recapture events in this study was limited ($n = 22$). However, the marmot population investigated by Corlatti et al. (2017) had a similar capture history (62 capture events, 39 individually marked animals and 23 recaptures) and the results of classic CMR models were consistent with mark–resight estimates, which were based on a much higher number of recaptures than CMR, and relied on fewer assumptions (i.e. no need for equal resighting probability among individuals and no need for independence among sighting events). This, in turn supports the use of CMR to estimate marmot populations despite the limited number of recapture events.

Overall, the source of bias causing CTDS (and, consequently, line DS) to underestimate population size compared to CMR, despite availability correction, remains unclear. We cannot exclude that some predation events by the golden eagle *Aquila chrysaetos* or the red fox *Vulpes vulpes* might have occurred between the CMR (6–16 June), CTDS (23–30 June) and DS (2–7 July) sessions, but the timeframe seems too short to explain such a difference through predation. Next, the use of classic CMR estimators makes the comparison with DS difficult, as CMR estimates population size, while distance sampling estimates density. While the use of spatially explicit capture–recapture models (SECR; Royle et al. 2014) would be desirable for comparison, preliminary SECR analyses returned unreliable estimates and a classic CMR approach was therefore preferred. Although the use of a buffer around the trap grid is an arguably coarse approach to approximate the effective trapped area (cf. White et al. 1982), preliminary inspection of marmot movements between traps (that is, the occurrence of capture events of the same individuals in different traps) revealed that only one individual was captured in two adjacent traps, 79 m apart (on top of Fig. 1c). This suggests limited movements of individuals outside their territories during the CMR sampling session, thereby supporting the use of the 83 m buffer width to approximate the effective trapped area. In turn, this should make the (CT)DS–CMR comparison possible. We thus believe the difference between availability bias-corrected (CT)DS estimators and CMR estimators may be largely attributed to violations of assumptions underlying distance sampling methods, and to incorrect assessment of animal availability. Both line DS and CTDS likely violated the assumption of perfect detection at distance zero; consequently, this should lead to low estimates compared to

CMR. Furthermore, estimates of animal availability using activity data crucially assume that at the peak of the daily activity cycle all animals are active (Rowcliffe et al. 2014). If the proportion of time spent being active overestimates the proportion of time spent by marmots being outside of burrows, then $P_{\text{availability}}$ would also be overestimated, thereby leading to underestimates of population size (cf. Cappelle et al. 2019). We are not aware of studies that assessed if, at a given time of day, all marmots are active outside of burrows. Our field experience in observing marked individuals suggests that the simultaneous presence of all animals outside of burrows is highly unlikely. If so, we suggest that the discrepancy between CMR and distance sampling estimators may be largely due to overestimation of availability. Lastly, we acknowledge that the limited sample size in this study might also have hampered our ability to make strong inferences regarding the accuracy of estimators, and possibly the sources of bias that caused estimates to differ.

Conclusions

When true population size is unknown, between-methods comparisons are difficult. Yet, we argue that CMR estimators are more likely to approximate true population size than DS methods, in marmots, as CMR appears less sensitive than (CT)DS to violation of assumptions caused by the behavior of this species, especially with respect to issues of temporally limited availability.

If DS methods are applicable without serious violation of assumptions, line DS and CTDS return similar results, but the former is likely to be more reliable and cost-effective than the latter. Although the use of camera traps may allow to reduce field effort, CTDS drastically increases the number of desk-work hours for photo/video-processing, an issue that may be important considering the need to deploy a substantial number of devices to improve the precision of the estimator (cf. Howe et al. 2017, Cappelle et al. 2019 and this study). Future studies should explicitly explore the trade-off between the costs and benefits of CTDS versus alternate methods, possibly including a power analysis to assess the number of cameras needed to achieve the desired level of precision.

Although CTDS severely underestimated population size in our study population, we suggest that if violations of assumptions can be excluded, CTDS may be a promising method when the aim is to estimate absolute population size. To reduce the risk of violating CTDS assumptions, we suggest to set up cameras in video mode, as in Howe et al. (2017) and Cappelle et al. (2019), and record distances at each predefined snapshot moment, e.g. every 2 s. This allows to choose t , rather than rely on settings that cannot be changed. If researchers or wildlife managers prefer to use single still images, consistency check of user-manual versus empirical θ and t^* is crucial to avoid biased estimators. In any case, proper availability-bias corrections will always need to be considered when using CTDS (Howe et al. 2017).

Acknowledgements – We thank Stephen Buckland, Eric Rexstad, Eric Howe (Univ. of St. Andrews), Jim-Lino Kämmerle (Univ. of

Freiburg), Lorenzo Fattorini (Univ. of Siena), and the Editor Wibke Peters for insightful comments on earlier drafts of the manuscript. *Funding* – The article processing charge was funded by the German Research Foundation (DFG) and the University of Freiburg in the funding programme Open Access Publishing.

References

- Armitage, K. B. 2014. Marmot biology: sociality, individual fitness and population dynamics. – Cambridge Univ. Press.
- Bessone, M. et al. 2020. Drawn out of the shadows: surveying secretive forest species with camera trap distance sampling. – *J. Appl. Ecol.* 57: 963–974.
- Borchers, H. W. 2019. *pracma*: practical numerical math functions. – R package ver. 2.2.9. <<https://CRAN.R-project.org/package=pracma>>.
- Buckland, S. T. et al. 2001. Introduction to distance sampling. – Oxford Univ. Press.
- Buckland, S. T. et al. 2007. Line transect methods for plant surveys. – *Biometrics* 63: 989–998.
- Buckland, S. T. et al. 2015. Distance sampling: methods and applications. – Springer.
- Burnham, K. P. and Anderson, D. R. 2002. Model selection and multimodel inference, 2 edn. – Springer.
- Cappelle, N. et al. 2019. Validating camera trap distance sampling for chimpanzees. – *Am. J. Primatol.* 81: e22962.
- Chandler, R. B. and Royle, J. A. 2013. Spatially explicit models for inference about density in unmarked or partially marked populations. – *Ann. Appl. Stat.* 7: 936–954.
- Corlatti, L. et al. 2017. A comparison of four methods to estimate population size of Alpine marmot (*Marmota marmota*). – *Hystrix* 28: 61–67.
- Fryxell, J. M. et al. 2014. Wildlife ecology, conservation and management. – Wiley Blackwell.
- Greenwood, J. J. D. and Robinson, R. A. 2006. General census methods. – In: Sutherland, W. J. (ed.), *Ecological census techniques: a handbook*. Cambridge Univ. Press, pp. 87–185.
- Hofmeester, T. R. et al. 2017. A simple method for estimating the effective detection distance of camera traps. – *Remote Sens. Ecol. Conserv.* 3: 81–89.
- Howe, E. J. et al. 2017. Distance sampling with camera traps. – *Methods Ecol. Evol.* 8: 1558–1565.
- Howe, E. J. et al. 2019. Model selection with overdispersed distance sampling data. – *Methods Ecol. Evol.* 10: 38–47.
- Huggins, R. 2001. A note on the difficulties associated with the analysis of capture–recapture experiments with heterogeneous capture probabilities. – *Stat. Prob. Lett.* 4: 147–152.
- Jathanna, D. et al. 2003. Estimation of large herbivore densities in the tropical forests of southern India using distance sampling. – *J. Zool.* 261: 285–290.
- Kendall, W. L. 1999. Robustness of closed capture–recapture methods to violations of the closure assumption. – *Ecology* 80: 2517–2525.
- Laake, J. L. 2013. RMark: an R interface for analysis of capture–recapture data with MARK. – AFSC Processed Rep. 2013-01. Alaska Fish. Sci. Cent., NOAA, Natl. Mar. Fish. Serv., Seattle, WA.
- Marques, T. A. et al. 2007. Improving estimates of bird density using multiple-covariate distance sampling. – *Auk* 124: 1229–1243.
- Marques, T. A. et al. 2013. Estimating animal population density using passive acoustics. – *Biol. Rev.* 88: 287–309.
- Miller, D. L. et al. 2019. Distance sampling in R. – *J. Stat. Softw.* 89: 1–28.
- Moeller, A. K. et al. 2018. Three novel methods to estimate abundance of unmarked animals using remote cameras. – *Ecosphere* 9: e02331.
- Nichols, J. D. et al. 2009. Inferences about landbird abundance from count data: recent advances and future directions. – In: Thompson, D. L. et al. (eds), *Modeling demographic processes in marked populations*. Springer, pp. 201–235.
- O'Donnell, K. M. et al. 2015. Partitioning detectability components in populations subject to within-season temporary emigration using binomial mixture models. – *PLoS One* 10: e0117216.
- Otis, D. L. et al. 1978. Statistical inference from capture data on closed animal populations. – *Wildl. Monogr.* 62: 3–135.
- Pollock, K. H. et al. 2002. Large scale wildlife monitoring studies: statistical methods for design and analysis. – *Environmetrics* 13: 105–119.
- Ridout, M. and Linkie, M. 2009. Estimating overlap of daily activity patterns from camera trap data. – *J. Agric. Biol. Environ. Stat.* 14: 322–337.
- Rovero, F. and Zimmermann, F. 2016. Camera trapping for wildlife research. – Pelagic Publishing.
- Royle, J. A. 2004. N-mixture models for estimating population size from spatially replicated counts. – *Biometrics* 60: 108–115.
- Royle, J. A. et al. 2014. Spatial capture–recapture. – Academic Press.
- Rowcliffe, J. M. et al. 2008. Estimating animal density using camera traps without the need for individual recognition. – *J. Appl. Ecol.* 45: 1228–1236.
- Rowcliffe, J. M. et al. 2011. Quantifying the sensitivity of camera traps: an adapted distance sampling approach. – *Methods Ecol. Evol.* 2: 464–476.
- Rowcliffe, J. M. et al. 2014. Quantifying levels of animal activity using camera trap data. – *Methods Ecol. Evol.* 5: 1170–1179.
- RStudio Team 2019. RStudio: integrated development for R. – RStudio Inc., Boston, MA.
- Ruette, S. et al. 2003. Applying distance-sampling methods to spotlight counts of red foxes. – *J. Appl. Ecol.* 40: 32–43.
- Schmidt, J. H. et al. 2017. Using non-invasive mark–resight and sign occupancy surveys to monitor low-density brown bear populations across large landscapes. – *Biol. Conserv.* 207: 47–54.
- Schwarz, C. J. and Seber, G. A. F. 1999. Estimating animal abundance: review III. – *Stat. Sci.* 14: 427–456.
- Sebastián-González, E. et al. 2018. Density estimation of sound-producing terrestrial animals using single automatic acoustic recorders and distance sampling. – *Avian Conserv. Ecol.* 13: 7.
- Seber, G. A. F. 1982. The estimation of animal abundance and related parameters, 2nd edn. – Griffin.
- Senar, J. C. et al. 1999. Identifying sources of heterogeneity in capture probabilities: an example using the great tit *Parus major*. – *Bird Study* 46: S248–S252.
- Séquin, E. S. et al. 2003. Wariness of coyotes to camera traps relative to social status and territory boundaries. – *Can. J. Zool.* 81: 2015–2025.
- Spiess, A.-N. 2018. propagate: propagation of uncertainty. – R package ver. 1.0-6.
- Thomas, L. et al. 2010. Distance software: design and analysis of distance sampling surveys for estimating population size. – *J. Appl. Ecol.* 47: 5–14.
- Thompson, W. L. et al. 1998. Monitoring vertebrate populations. – Academic Press.
- White, G. C. 2008. Closed population estimation models and their extensions in Program MARK. – *Environ. Ecol. Stat.* 15: 89–99.
- White, G. C. et al. 1982. Capture–recapture and removal methods for sampling closed populations. – Los Alamos National Laboratory.
- Williams, B. K. et al. 2002. Analysis and management of animal populations. – Academic Press.
- Yoccoz, N. G. et al. 2001. Monitoring of biological diversity in space and time. – *Trends Ecol. Evol.* 16: 446–453.
- Zerbini, A. N. et al. 2007. Estimating abundance of killer whales in the nearshore waters of the Gulf of Alaska and Aleutian Islands using line-transect sampling. – *Mar. Biol.* 150: 1033–1045.